Astron. Astrophys. 279, 668–673 (1993)

ASTRONOMY
AND
ASTROPHYSICS

Series inversion of Abel equation for very peaked profiles: the $R^{1/4}$–law

O. Bendinelli[1], **L. Ciotti**[2,3], **and G. Parmeggiani**[2]

[1] Dipartimento di Astronomia, Università di Bologna, via Zamboni 33, I-40126 Bologna, Italy
[2] Osservatorio Astronomico di Bologna, via Zamboni 33, I-40126 Bologna, Italy
[3] Princeton University Observatory, Peyton Hall, Princeton NJ, USA

Received June 1, accepted July 5, 1993

Abstract. The series expansion by gaussian or exponential functions of a brightness profile (given in numerical or analytical form), supplies an easy and accurate way to derive its spatial deprojection, also in the form of series, thus by–passing the numerical difficulties related to the direct solution of the Abel integral equation. In this paper we consider in particular the problem of the Abel inversion when the unprojected density profile is highly peaked (or divergent) in the center. Under the assumption of the exponential function as "basis" for the expansions, the unprojected density is obtained as a sum of Bessel functions. The expressions for the most used properties of a spherical model are then derived. The capability of exponentials to reproduce peaked density distributions, with respect to a gaussian expansion, is shown by the application of the exponential expansion to the $R^{1/4}$ profile. Many other basic properties of this profile are expanded in the gaussian and exponential basis, and the coefficients are given.

Key words: methods: analytical – methods: data analysis – galaxies: elliptical

1. Introduction

The importance of obtaining the spatial density ρ from the surface brightness profile Σ of a stellar system – also in the rough approximation of spherical symmetry – is so great in galactic dynamics (realistic model construction, interpretation of observations, both of brightness profile and velocity dispersion) that it is not necessary to discuss extensively this point (for a presentation of the subject see e.g. Binney & Tremaine 1987), but only to present the formal problem.

In spherical systems the space light density $\nu(r)$ and the surface brightness $\Sigma(R)$ are related by the Abel integral equation

$$\Sigma(R) = 2\int_R^\infty \frac{r\nu(r)dr}{\sqrt{r^2-R^2}}, \tag{1}$$

Send offprint requests to: L. Ciotti

whose analytical inversion reads as

$$\nu(r) = -\frac{1}{\pi}\int_r^\infty \frac{d\Sigma(R)}{dR}\frac{dR}{\sqrt{R^2-r^2}}, \tag{2}$$

and where r and R are the spatial and the projected radii, respectively. In evaluating the previous equation we distinguish 3 cases.

The easiest (and least common) situation is represented by the family of profiles for which Eq. (2) can be solved in closed form. It is well known that the $R^{1/4}$–law (de Vaucouleurs 1948), that give a remarkable fit of the surface brightness distribution of ellipticals and bulges, doesn't belong to this family.

The second possibility is the direct inversion, i.e. the direct numerical solution of the integral equation. In this case, when the surface brightness is given as a (non invertible) function, there are no particular problems in deriving the light density by numerical integration of Eq. (2), apart from some caution with the central (weak) singularity of the deprojection kernel. Usually this problem can be solved by integrating by parts Eq. (2). This was done, for instance, by Poveda et al.(1960) and Young (1976) dealing with the de Vaucouleurs profile, or more recently for the generalized $R^{1/m}$ models by one of us (Ciotti 1991). Much more challenging is the density derivation from a surface brightness profile expressed in tabular form, because in this case the numerical differentiation cannot give the accurate approximation of the derivative required by Eq. (2). In this case the numerical integration of Eq. (2) may be performed by the algebraic approach (i.e. the discretization by a large linear system, see e.g. Bendinelli et al.1977), by Fourier or other type of transforms. The computational difficulty of Abel numerical inversion, which belongs to the class of unstable inverse problems and occurs in all fields of applied sciences, is well depicted in the Gorenflo & Vessella monography (1991), or in that by Craig & Brown (1986) devoted to the astronomical field. It must be pointed out that it is not easy to use the numerical light density obtained in both the above cases in applications such as a model construction (calculations of potential, potential energy, fractional mass, etc.) and its comparison with observations.

© European Southern Observatory • Provided by the NASA Astrophysics Data System

The third way to derive the light density, sporadically used in the past (see for instance Oort & van Herk 1959; Capaccioli 1980), is indirect and based on the expansion of the surface brightness $\Sigma(R)$ in a truncated series of positive functions for which Eq. (2) can be inverted analytically: this is the approach we use here. In the first part of this paper we address the general problem of the inversion, via (finite) series expansion (in gaussian and exponential basis) of peaked density distributions. For these expansions in Sect. 2 we give the general formulae for the fundamental quantities, and in Sect. 3 we discuss extensively the particular case of the $R^{1/4}$–law. In the second part of this paper we give the explicit expansion's coefficients for the density, potential, mass inside the radius r, spatial and projected velocity dispersion (in the case of global isotropy) for this law. Finally in Sect. 4 we shortly discuss the results.

2. Gaussian and exponential expansions: general properties

2.1. The Abel integral equation and the spatial light density

We start analyzing the formal properties of the expansion in gaussian and exponential functions of a surface brightness profile. So we assume:

$$\Sigma(R) = \frac{L_T}{R_e^2} \sum_{i=1}^{N} \frac{a_i}{2\pi\alpha_i^2} \exp(-\eta^2/2\alpha_i^2), \tag{3}$$

or

$$\Sigma(R) = \frac{L_T}{R_e^2} \sum_{i=1}^{N} \frac{a_i}{2\pi\alpha_i^2} \exp(-\eta/\alpha_i), \tag{4}$$

where a_i and α_i are positive constants, L_T is the total luminosity, R_e is some characteristic radius of the distribution (here is the effective radius), $\eta = R/R_e$, and N (generally small) is the number of terms sufficient to give a good approximation of the starting profile. The dispersions α_i are normalized to R_e and the coefficients a_i are dimensionless constants. It is important to stress that in Eqs. (3) and (4) the conservation of the total luminosity requires that

$$\sum_{i=1}^{N} a_i = 1. \tag{5}$$

The given normalization and positivity relations are fundamental for the consistency of the expansions. The parameters a_i and α_i are easily computable using the Newton–Gauss regularized method (Bendinelli et al.1987; Bendinelli 1991), which is a powerful iterative non linear fitting technique (but when the data are obtainable in specified points of a smooth distribution, much simpler procedures can be used, as pointed out in the above papers). Inserting the derivatives of Eqs. (3) and (4) in the right–hand side of Eq. (2) the expressions for the density result respectively:

$$\nu(r) = \frac{L_T}{R_e^3} \sum_{i=1}^{N} \frac{a_i}{(2\pi)^{3/2}\alpha_i^3} \exp(-s^2/2\alpha_i^2), \tag{6}$$

and

$$\nu(r) = \frac{L_T}{R_e^3} \sum_{i=1}^{N} \frac{a_i}{2\pi^2\alpha_i^3} \mathrm{K}_0(s/\alpha_i), \tag{7}$$

where $s = r/R_e$ and K_0 is the modified Bessel function of zeroth order. The proof of Eq. (6) is straightforward while for Eq. (7) see formula 8.432.3 in Gradshstein & Ryzhik (1965, hereafter GR).

Regarding the use of gaussians or exponentials in the expansion of a profile, we can expect that, due to the central divergence of the Bessel functions, the first type of functions is more suitable (i.e. less terms are needed) when the profile is flat towards the centre, the last when it is more cuspy. We show in the next section the correctness of this statement inverting the $R^{1/4}$ profile. We conclude this general discussion by obtaining some other general formulae using the profile expansion of the surface brightness profile. Very rapidly the formulae become intractable, due to the successive integrals required. Then, for practical purposes, we expand each basic function associated with the $R^{1/4}$–law (mass, potential, velocity dispersion) both in gaussian and exponential functions, giving the associated coefficients.

2.2. Integrated luminosity

Integrated luminosities are other important properties that can be formally derived from series expansions. We first consider the projected luminosity inside the cylinder of radius R centered on the system, which by definition is $L_P(R) = 2\pi \int_0^R x\Sigma(x)dx$. By simple integration the explicit expression of L_P for the gaussian and exponential expansion reads respectively as

$$\Delta L_P(R) \equiv L_T - L_P(R) = \sum_{i=1}^{N} a_i \exp(-\eta^2/2\alpha_i^2)], \tag{8}$$

and

$$\Delta L_P(R) = \sum_{i=1}^{N} a_i \left(1 + \frac{\eta}{\alpha_i}\right) \exp(-\eta/\alpha_i). \tag{9}$$

Clearly for $R \to \infty$ the total luminosity is recovered in both cases, i.e. $\Delta L_P(\infty) = 0$.

The total luminosity contained in the sphere of radius r is instead obtained by volume integration of Eqs. (6) and (7), i.e. $L(r) = 4\pi \int_0^r x^2\nu(x)dx$, obtaining for the gaussian expansion

$$L(r) = L_T \sum_{i=1}^{N} a_i \left[\Phi\left(\frac{s}{\sqrt{2}\alpha_i}\right) - \sqrt{\frac{2}{\pi}} \frac{s}{\alpha_i} \exp(-s^2/2\alpha_i^2)\right] \tag{10}$$

where $\Phi(x) \equiv 2/\sqrt{\pi} \int_0^x \exp(-t^2)dt$ (GR-8.250.1). As far as the exponential expansion is concerned, the evaluation of Eq. (10) is more complicated and requires an integration by parts and the

© European Southern Observatory • Provided by the NASA Astrophysics Data System

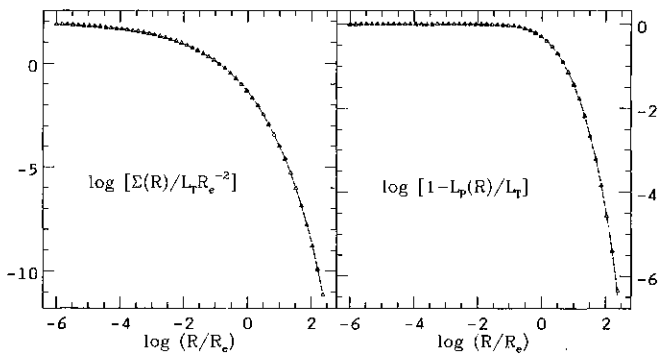

Fig. 1. Left panel: the de Vaucouleurs profile (triangles) with gaussian (dashed line) and exponential (dotted line) expansions, in the Young radial range. All the profiles are normalized to L_T/R_e^2. Right panel: comparison of the functions $\Delta L_P(R)/L_T$, for the de Vaucouleurs law and its gaussian and exponential expansions. Note that the two expansions are exactly superimposed

use of formulae GR-8.472.3 and GR-6.561.4, getting as final result:

$$L(r) = L_T \sum_{i=1}^{N} \frac{a_i s}{\alpha_i} \Big\{ \Big[\mathrm{K_1}\Big(\frac{s}{\alpha_i}\Big)\mathbf{L_0}\Big(\frac{s}{\alpha_i}\Big) + \mathbf{K_0}\Big(\frac{s}{\alpha_i}\Big)\mathbf{L_1}\Big(\frac{s}{\alpha_i}\Big)\Big] - \frac{2}{\pi}\frac{s}{\alpha_i}\mathbf{K_1}\Big(\frac{s}{\alpha_i}\Big)\Big\} \tag{11}$$

where $\mathrm{K_1}$ is the modified Bessel function of first order, and $\mathbf{L_n}$ are the modified Struve functions (GR-8.551.2).

3. An example: the de Vaucouleurs profile

3.1. Surface brightness

The previous formulae have the characteristic of being completely general, but still require some numerical work (e.g. numerical integration) to be implemented in numerical codes for applications. So, in this section we give the radial expansion for the most important functions associated with the $R^{1/4}$–law, derived by expansion of the true functions in gaussian and exponential sums. We choose this profile for three reasons. The first is the apparent uniformity of luminosity profiles in hot stellar systems, described by the $R^{1/4}$-law, the second is that this law is a non–invertible function very peaked in the center, i.e. an ideal candidate for the expansion technique and for testing the superiority of exponential functions in this case. We have finally another important property of the de Vaucouleurs profile, i.e. the absence of free parameters, from which for a given type of basis functions and physical scales of the profiles (e.g. L_T and R_e), the expansion coefficients are determined unequivocally. The expansion of the $R^{1/4}$–law surface brightness profile (as well as its other properties presented in this paper),

$$\Sigma(R) = \Sigma_\circ \exp(-b\eta^{1/4}) \tag{12}$$

(where $b = 7.6672489...$) by gaussian and exponential functions is performed over the radial range used in Young's calculations,

Table 1. Parameters of gaussian (left) and exponential (right) expansions for the $R^{1/4}$ profile normalized to L_T/R_e^2 in the range $10^{-6} \leq \eta \leq 240$

N	a_i	α_i	a_i	α_i
1	$2.440\ 10^{-10}$	$1.987\ 10^{-6}$	$1.191\ 10^{-8}$	$9.512\ 10^{-6}$
2	$2.396\ 10^{-8}$	$1.564\ 10^{-5}$	$8.555\ 10^{-6}$	$2.321\ 10^{-4}$
3	$1.596\ 10^{-6}$	$1.240\ 10^{-4}$	$7.997\ 10^{-4}$	$2.708\ 10^{-3}$
4	$4.586\ 10^{-5}$	$7.308\ 10^{-4}$	$1.472\ 10^{-2}$	$1.698\ 10^{-2}$
5	$6.155\ 10^{-4}$	$3.236\ 10^{-3}$	$8.730\ 10^{-2}$	$7.114\ 10^{-2}$
6	$4.459\ 10^{-3}$	$1.142\ 10^{-2}$	$2.253\ 10^{-1}$	$2.280\ 10^{-1}$
7	$1.960\ 10^{-2}$	$3.384\ 10^{-2}$	$3.050\ 10^{-1}$	$6.114\ 10^{-1}$
8	$5.695\ 10^{-2}$	$8.753\ 10^{-2}$	$2.363\ 10^{-1}$	$1.461\ 10^{0}$
9	$1.163\ 10^{-1}$	$2.032\ 10^{-1}$	$1.049\ 10^{-1}$	$3.235\ 10^{0}$
10	$1.744\ 10^{-1}$	$4.321\ 10^{-1}$	$2.560\ 10^{-2}$	$6.802\ 10^{0}$
11	$1.987\ 10^{-1}$	$8.548\ 10^{-1}$	$3.105\ 10^{-3}$	$1.397\ 10^{1}$
12	$1.768\ 10^{-1}$	$1.590\ 10^{0}$	$1.323\ 10^{-4}$	$2.983\ 10^{1}$
13	$1.258\ 10^{-1}$	$2.809\ 10^{0}$	—	—
14	$7.314\ 10^{-2}$	$4.757\ 10^{0}$	—	—
15	$3.509\ 10^{-2}$	$7.801\ 10^{0}$	—	—
16	$1.376\ 10^{-2}$	$1.252\ 10^{1}$	—	—
17	$4.320\ 10^{-3}$	$1.980\ 10^{1}$	—	—
18	$1.052\ 10^{-3}$	$3.119\ 10^{1}$	—	—
19	$1.839\ 10^{-4}$	$4.989\ 10^{1}$	—	—
20	$1.744\ 10^{-5}$	$8.604\ 10^{1}$	—	—

i.e. $10^{-6} \leq R/R_e \leq 240$. The goodness of the fits [parameters in Table 1, see also Fig. (1)], are clearly seen.

We remember that the relation $L_T = 8!\pi b^{-8}\,\Sigma_\circ R_e^2 \simeq 1.058 \times 10^{-2}\,\Sigma_\circ R_e^2$ holds (e.g. Ciotti 1991). A comment is in order for numerical applications of Eqs. (8) and (9): for very small radii it is better to use the first order expansion of the exponential functions, due to the difference between very similar quantities.

3.2. Spatial light density

Having the coefficients of the profile expansions, we have also the spatial density distribution given by Eqs. (6) and (7). It is easy to see that the numerical values given by these expansions are a very good approximation for the $R^{1/4}$ spatial density in the interpolation range, better for example than the Mellier & Mathez (1987) formula in the central regions [Fig. (2)].

Moreover the agreement should be further improved towards the centre because parameters have been obtained by an automatic (and so not "ad hoc") procedure giving the initial values required by Newton–Gauss iteration.

Many times very simple formulae are required working with the $R^{1/4}$–law, not only for the spatial density but e.g. for the mass inside the radius r, the potential, the velocity dispersion. From this point of view the Bessel functions are certainly worse than the Mellier and Mathez approximation. This latter approximation however fails in satisfying the simplicity criteria required by

© European Southern Observatory • Provided by the NASA Astrophysics Data System

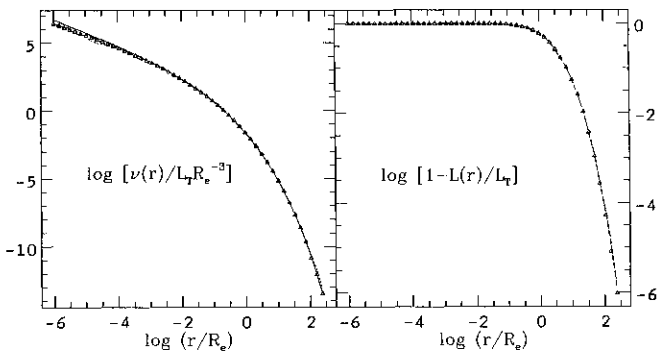

Fig. 2. Left panel: comparison of the light densities, normalized to L_T/R_e^3 for the de Vaucouleurs law (triangles), gaussian (dashed line) exponential (dotted line) expansions, and the Mellier and Mathez formula (solid line). Right panel: comparison of the functions $\Delta L(r)/L_T$, for the de Vaucouleurs law and its gaussian and exponential expansions

Table 2. Parameters of exponential expansion of the density associated to the $R^{1/4}$ profile, normalized to L_T/R_e^3 in the range $10^{-6} \leq \eta \leq 240$

N	b_i	β_i
1	$3.409\ 10^{-9}$	$3.753\ 10^{-6}$
2	$4.908\ 10^{-6}$	$1.234\ 10^{-4}$
3	$6.370\ 10^{-4}$	$1.691\ 10^{-3}$
4	$1.473\ 10^{-2}$	$1.198\ 10^{-2}$
5	$1.402\ 10^{-1}$	$6.549\ 10^{-2}$
6	$2.750\ 10^{-1}$	$2.324\ 10^{-1}$
7	$3.199\ 10^{-1}$	$6.614\ 10^{-1}$
8	$1.952\ 10^{-1}$	$1.635\ 10^{0}$
9	$7.191\ 10^{-2}$	$3.656\ 10^{0}$
10	$1.292\ 10^{-2}$	$8.164\ 10^{0}$
11	$5.277\ 10^{-4}$	$2.188\ 10^{1}$
12	$1.326\ 10^{-4}$	$2.740\ 10^{1}$

applications. So we expand in gaussians and exponential functions many properties associated with the de Vaucouleurs law. We call the parameters of the density expansion b_i and β_i, and from Eq. (6) it results that for the gaussian expansion $b_i = a_i$ and $\beta_i = \alpha_i$. For the exponential interpolation, with the usual convention that the sum of the coefficients b_i is 1, we have:

$$\nu(r) = \frac{L_T}{R_e^3} \sum_{i=1}^{N} \frac{b_i}{8\pi\beta_i^3} \exp(-s/\beta_i), \tag{13}$$

where b_i are given in Table 2.

3.3. Luminosity inside r

For what concerns the spatial luminosity profile, Eqs. (11) and (12) are not of immediate use. So we expand the profile in the

Table 3. Parameters of gaussian (left) and exponential (right) expansion of $\Delta L(r)/L_T$ associated with the $R^{1/4}$ profile, in the range $10^{-6} \leq \eta \leq 240$

N	c_i	γ_i	c_i	γ_i
1	$5.272\ 10^{-2}$	$4.712\ 10^{-2}$	$4.175\ 10^{-2}$	$1.263\ 10^{0}$
2	$3.573\ 10^{-1}$	$4.262\ 10^{-1}$	$5.330\ 10^{-1}$	$1.269\ 10^{0}$
3	$3.743\ 10^{-1}$	$1.757\ 10^{0}$	$3.605\ 10^{-1}$	$3.977\ 10^{0}$
4	$1.621\ 10^{-1}$	$4.870\ 10^{0}$	$6.828\ 10^{-2}$	$1.065\ 10^{1}$
5	$4.449\ 10^{-2}$	$1.084\ 10^{1}$	$2.095\ 10^{-3}$	$2.763\ 10^{1}$
6	$8.054\ 10^{-3}$	$2.176\ 10^{1}$	$3.618\ 10^{-4}$	$4.130\ 10^{1}$
7	$8.893\ 10^{-4}$	$3.582\ 10^{1}$	—	—
8	$2.413\ 10^{-4}$	$5.931\ 10^{1}$	—	—
9	$1.776\ 10^{-5}$	$1.031\ 10^{2}$	—	—

two bases, the coefficients being c_i and γ_i. Using the radial behaviour of the basis we expand the difference:

$$\Delta L(r) \equiv L_T - L(r) = L_T \sum_{i=1}^{N} c_i \exp(-s^2/2\gamma_i^2), \tag{14}$$

where for the exponential basis a totally similar equation holds. Again, the sum of the dimensionless coefficients is equal to 1. The expansion parameters are given in Table 3.

3.4. Potential

In the assumption of constant mass-to-light ratio $\mathscr{L}$, the potential can be immediately computed from the Gauss Theorem. The formulae derived from the density or luminosity interpolations are not elementary functions, so we give the expansions, in terms of parameters d_i and δ_i, of the absolute value of the potential, $\Psi(r)$. For the gaussian basis we have:

$$\Psi(r) = G\mathscr{L} \int_r^\infty \frac{L(r')}{r'^2} dr' = \Psi_\circ \sum_{i=1}^{N} d_i \exp(-s^2/2\delta_i^2), \tag{15}$$

where a totally analogous formula holds for the exponential expansion. Clearly the sum of the coefficients d_i has to be equal to 1, and the central potential is related to L_T ad R_e by the exact relation $\Psi_\circ = G\mathscr{L}\Sigma_\circ R_e 4b^{-4}4! \simeq 2.937 \times 10^{-4} G\mathscr{L} L_T R_e^{-1}$ (Ciotti 1991). Given the two expansions it is immediate to obtain the expression for the gravitational energy of the system:

$$\begin{aligned} |W| &= \frac{1}{2}\int_0^\infty 4\pi r^2 \rho(r)\Psi(r)\, dr \\ &= \frac{L_T \Psi_\circ \mathscr{L}\pi}{2} \sum_{i,j=1}^{N} \frac{b_i d_j \delta_j^3}{(\beta_i^2 + \delta_j^2)^{3/2}} \\ &= \frac{L_T \Psi_\circ \mathscr{L}}{2} \sum_{i,j=1}^{N} \frac{b_i d_j \delta_j^3}{(\beta_i + \delta_j)^3} \end{aligned} \tag{16}$$

© European Southern Observatory • Provided by the NASA Astrophysics Data System

Table 4. Parameters of gaussian (left) and exponential (right) expansions for the normalized potential of the $R^{1/4}$–law, $\Psi(r)/\Psi_o$, in the range $10^{-6} \leq s \leq 240$

N	d_i	δ_i	d_i	δ_i
1	$1.223\ 10^{-3}$	$3.442\ 10^{-5}$	$5.060\ 10^{-1}$	$1.166\ 10^{-1}$
2	$3.679\ 10^{-2}$	$1.359\ 10^{-3}$	$3.301\ 10^{-1}$	$1.042\ 10^{0}$
3	$1.962\ 10^{-1}$	$1.906\ 10^{-2}$	$1.040\ 10^{-1}$	$4.118\ 10^{0}$
4	$3.416\ 10^{-1}$	$1.419\ 10^{-1}$	$3.314\ 10^{-2}$	$1.328\ 10^{1}$
5	$2.560\ 10^{-1}$	$7.020\ 10^{-1}$	$1.115\ 10^{-2}$	$4.192\ 10^{1}$
6	$1.115\ 10^{-1}$	$2.684\ 10^{0}$	$4.249\ 10^{-3}$	$2.474\ 10^{2}$
7	$3.731\ 10^{-2}$	$8.648\ 10^{0}$	—	—
8	$1.255\ 10^{-2}$	$2.510\ 10^{1}$	—	—
9	$4.233\ 10^{-3}$	$6.959\ 10^{1}$	—	—
10	$2.629\ 10^{-3}$	$2.468\ 10^{2}$	—	—

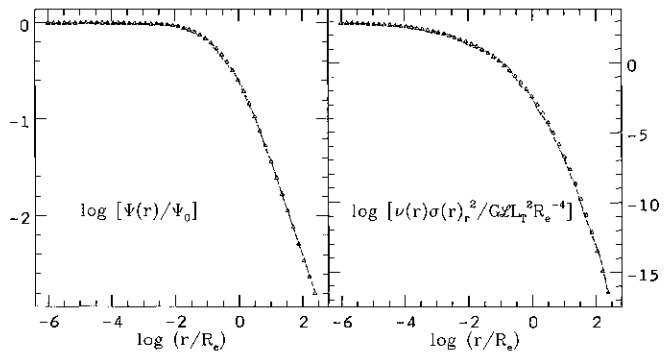

Fig. 3. Left panel: comparison of the potential, normalized to the central value, for the de Vaucouleurs law (triangles), gaussian (dashed line) and exponential (dotted line) expansions. Right panel: the product $\nu(r)\sigma_r^2(r)$ normalized to $G\mathscr{L}L_T^2/R_e^4$, compared with the gaussian and exponential expansions

where the first expression holds for the gaussian expansion and the second for the exponential one. The expansion parameters are reported in Table 4.

3.5. Isotropic velocity dispersion

The last function we describe is the spatial velocity dispersion profile, in the particular case of a global isotropy of the velocity dispersion tensor. So we expand the well known formula

$$\nu(r)\sigma_r^2(r) = G\mathscr{L}\int_r^\infty \frac{\nu(r')L(r')\,dr'}{r'^2} = \frac{G\mathscr{L}L_T^2}{R_e^4}\sum_{i=1}^{N} e_i \exp(-s^2/2\epsilon_i^2) \tag{17}$$

and a totally similar formula holds for the exponential expansion. The values of the parameters are given in Table 5. We note

Table 5. Parameters of gaussian (left) and exponential (right) expansion of $\nu(r)\sigma_r^2(r)$ normalized to $G\mathscr{L}L_T^2/R_e^4$, associated to the $R^{1/4}$ profile in the range $10^{-6} \leq \eta \leq 240$ and in case of global isotropy of the velocity dispersion tensor

N	e_i	ϵ_i	e_i	ϵ_i
1	$1.144\ 10^{-7}$	$8.144\ 10^{-6}$	$1.164\ 10^{-5}$	$6.168\ 10^{-5}$
2	$1.181\ 10^{-4}$	$2.338\ 10^{-4}$	$1.174\ 10^{-2}$	$2.710\ 10^{-3}$
3	$8.657\ 10^{-3}$	$3.263\ 10^{-3}$	$1.643\ 10^{-1}$	$4.051\ 10^{-2}$
4	$6.480\ 10^{-2}$	$2.312\ 10^{-2}$	$8.158\ 10^{-2}$	$2.119\ 10^{-1}$
5	$1.500\ 10^{-1}$	$1.154\ 10^{-1}$	$5.468\ 10^{-3}$	$9.545\ 10^{-1}$
6	$4.029\ 10^{-2}$	$4.610\ 10^{-1}$	$8.724\ 10^{-5}$	$3.366\ 10^{0}$
7	$5.769\ 10^{-3}$	$1.436\ 10^{0}$	$2.437\ 10^{-7}$	$1.093\ 10^{1}$
8	$3.813\ 10^{-4}$	$3.903\ 10^{0}$	$1.439\ 10^{-8}$	$2.007\ 10^{1}$
9	$1.474\ 10^{-5}$	$9.275\ 10^{0}$	—	—
10	$3.679\ 10^{-7}$	$2.006\ 10^{1}$	—	—
11	$8.685\ 10^{-9}$	$4.869\ 10^{1}$	—	—
12	$1.328\ 10^{-10}$	$7.684\ 10^{1}$	—	—

that using the gaussian or the exponential basis it is impossible to recover the exact value of the central (isotropic) velocity dispersion, that for the $R^{1/4}$–law is 0 (Ciotti 1991). Finally we stress that in the case of the gaussian expansion it is straightforward to obtain a simple expression for the projected velocity dispersion profile:

$$\Sigma(r)\sigma_p^2(R) = \frac{G\mathscr{L}L_T^2}{R_e^3}\sqrt{\frac{\pi}{2}}\sum_{i=1}^{N} e_i\epsilon_i \exp(-\eta^2/2\epsilon_i^2), \tag{18}$$

4. Conclusions

Expansions by gaussian and exponential functions provide a useful tool for analysing observed profiles even if they are so undersampled and noisy that more mathematically correct or sophisticated numerical techniques cannot be used in deconvolution and deprojection problems.

The application to the de Vaucouleurs profile is here done first to check the feasibility and the accuracy of the method, and second to supply two approximations to the $R^{1/4}$ profile and its deprojection, together with many other properties useful in applications, and hence of aid in many areas of galactic research in which the de Vaucouleurs profile is widely employed.

Acknowledgements. We are grateful to the referee, J.C. Brown for helpful comments. One of us (L.C.) acknowledges S. Pellegrini and A. D'Ercole for useful discussions, and the hospitality of the Princeton University Observatory, where he was supported by the NSF grant AST9108103. This work was done under the financial support of the Ministero della Università e Ricerca Scientifica (MURST).

© European Southern Observatory • Provided by the NASA Astrophysics Data System

References

Bendinelli, O., 1991. ApJ, **366**, 599.

Bendinelli, O., Parmeggiani, G., & Lorenzutta, S., 1977. Mem.SAIt, **48**, 67.

Bendinelli, O., Parmeggiani, G., Piccioni,A., & Zavatti, F., 1987. AJ, **94**, 1095.

Binney, J., & Tremaine, S., 1987. *Galactic Dynamics*, Princeton University Press.

Capaccioli, M., 1980. Mem.SAIt, **51**, 497.

Ciotti, L., 1991. A&A, **249**, 99.

Craig, I.J.D., & Brown, J.C., 1986. *Inverse Problems in Astronomy*, (Bristol:Adam Hilger)

de Vaucouleurs, G., 1948. *Ann. d'Astroph.*, **11**, 247.

Gorenflo, R., & Vessella, S., 1991. *Abel Integral Equations*, (Berlin: Springer–Verlag), p.195

Gradshteyn, I.S., & Ryzhik, I.M., 1965. *Tables of Integrals Series and Products*, (London:Academic Press), p.958

Mellier, Y., & Mathez, G., 1987. A&A, **175**, 1.

Oort, J.H., & van Herk, G., 1959 *Bull. Astron. Inst. Neth.*, **14**, 229

Poveda, A., Iturriaga, R., & Orozoco, I., 1960. *Bull. Obs. Tonantzintla y Tacubaya*, **20**, 3.

Young, P.J., 1976. AJ, **81**, 807.

This article was processed by the author using Springer-Verlag TEX A&A macro package 1992.

© European Southern Observatory • Provided by the NASA Astrophysics Data System